Preview Control of an Electrodynamic Shaker using Explicit Receding Horizon Control

Yasuhiro Uchiyama * Takeshi Hatanaka ** Masayuki Fujita **

* IMV CORPORATION, Osaka, JAPAN, (e-mail:
uchiyama@imv.co.jp).
** Department of Mechanical and Control Engineering, Tokyo Institute
of Technology, Tokyo, JAPAN

Abstract: This paper addresses control of an electroadynamic shaker via explicit receding horizon preview control. In order to suppress effects of uncertainties including the state of test pieces on the shaker, we first design a local disturbance force compensator. Then, we form a two-degree-of-freedom controller so as to achieve an ideal tracking performance to acceleration references. In this paper, the feedforward controller is designed according to a model following design scheme, where the input generated by a state feedback controller stabilizing a plant model is applied as a reference input to the locally compensated system. In order to improve the tracking performance taking account of constraints which the system inherent possesses we employ as the state feedback controller a receding horizon control scheme including preview information on the reference signal. In particular, we use explicit receding horizon control computed through Multi-Parametric Toolbox for ease of implementation. Finally, the control performance is demonstrated through experiments on a testbed of a shaker system.

Keywords: Control applications; Robust control; Preview control; Vibration control; Actuators

1. INTRODUCTION

A lot of engineering products require vibration tests as one of durability tests and, for example in automotive industry, the tests are included into the process of production. Checking resistance of products against earthquakes also has highly important meanings especially in quake-prone Japan. For this purpose, electrodynamic shaking systems are widely used in the civil and architectural engineering as in Fig. 1 due to its good linearity and wide frequency responses. From the control engineers' point of view, the objective of the shaker system operation is to replicate some waveform (e.g. real data of earthquakes) in the presence of products on the shakers.

Control of shaking systems requires both of stable operations and good replication of the given reference acceleration waveform. It is known that robust vibration control is effective for the control problem and indeed several successful examples have been reported so far (Yano and Terashima, 2001; de Callafon et al., 2006; Lauwerys et al., 2005). However, if the interaction between the shaker and the test piece is not ignorable, the control of shaking systems becomes much more difficult especially in meeting test specifications rather than maintaining stability. Some researchers have addressed the issue so far (Iwasaki et al., 2005; Stoten and Shimizu, 2007). The authors also reported an attempt via disturbance-force compensator to suppress the effects of the disturbance force from the test pieces (Uchiyama and Fujita, 2010). However, we did not addressed explicitly improvement of tracking performances to actual reference acceleration waveforms.

2-degree-of-freedom (2DOF) control is widely accepted as a methodology to improve the tracking performances to the reference signal while compensating for the effects of uncertainties and disturbances. Indeed, a lot of practical successes have been reported (Jamaludin et al., 2009; Zimmermann and Sawodny, 2007). However, in addition to the acceleration tracking control, it is required for the shakers that the rated displacement of the electrodynamic shaker should not be greater than that of the other test equipments.

To deal with the inherent constraint in addition to a good tracking performance, we presented a novel control mechanism based on a model following type control scheme and an explicit receding horizon control (ERHC) (Hatanaka et al., 2008) in one of our previous works (Uchiyama et al., 2010). In the present scheme, the ERHC mechanism is embedded into the feedforward controller as a stabilizing state feedback controller of a plant model and the output of the controller is applied to the feedback control system as a reference input. In addition, we demonstrated the effectiveness of the present scheme through a testbed of the shaker system and constraint fulfillment was confirmed. However, we saw that the control error exceeds an acceptable level in order to meet the constraints. Therefore, in this paper, we focus on the fact that the future profile of the reference waveforms is in general available for control and apply a preview control scheme in order to improve the performance.

In this paper, we present a total control mechanism of electrodynamic shakers consisting of a disturbance-force
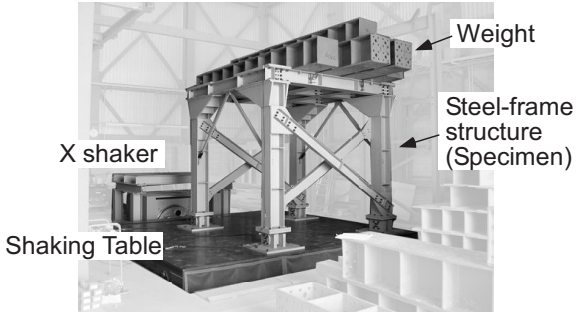
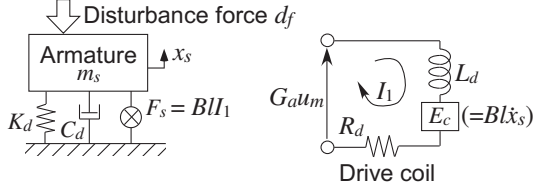Fig. 1. Multi-axis shaking system using the electrodynamic shakers.

Fig. 2. Schematic diagram of the armature and the equivalent circuit.

feedback compensator and a ERHC preview feedforward control. The rest of the paper is organized as follows: A mathematical model and an uncertainty weighting function are introduced in Section 2; A feedback controller is designed using μ-synthesis in Section 3; A preview control with the ERHC controller is constructed in Section 4; Section 5 provides experimental results; and finally the paper is summarized in Section 6.

2. ELECTRODYNAMIC SHAKER MODEL

2.1 Nominal model

Throughout this paper, we deal with an electrodynamic shaker depicted in Fig. 2. An electrodynamic force is generated in proportion to an electric current applied to the coil in the magnetic field. Assuming that the magnetic flux density is constant, a drive coil can be shown as a linear equivalent circuit. The schematic model of the shaker and the equivalent circuit are depicted in Fig. 2. The force F_s and the reverse electromotive force E_c can be represented as

$$F_s = BlI_1, \quad E_c = Bl\dot{x}_s, \quad (1)$$

where x_s denotes the displacement of the armature, I_1 denotes the current of the drive coil; l, the length of the drive coil; and B, the magnetic flux density, respectively. From Fig. 2, the equation

$$G_a u_m = R_d I_1 + L_d \dot{I}_1 + E_c \quad (2)$$

is obtained, where L_d denotes the inductance; R_d, the resistance; G_a, the amplifier gain; and u_m, the input voltage to the amplifier, respectively. The dynamic equation of the armature is described as

$$F_s = m_s\ddot{x}_s + C_d\dot{x}_s + K_d x_s, \quad (3)$$

where K_d denotes the stiffness coefficient of the suspension, and C_d denotes the damping coefficient of the suspension. The transfer function from the input voltage u_m to the acceleration $\ddot{x}_s$ can be represented as the state-space form

Table 1. Perturbed parameters and their ranges.

Symbol	Perturbed region
R_d	-10 – 10 %
L_d	-15 – 15 %
B	-10 – 10 %
G_a	-5 – 5 %
K_d	-10 – 10 %
C_d	-12 – 12 %
m_s	-9 – 9 %

$$\dot{x}_a = A_a x_a + B_a u_m, \quad y_m = C_a x_a,$$
$$x_a = [x_s \ \dot{x}_s \ I_1],$$
$$A_a = \begin{bmatrix} 0 & 1 & 0 \\ -\dfrac{K_d}{m_s} & -\dfrac{C_d}{m_s} & \dfrac{Bl}{m_s} \\ 0 & -\dfrac{Bl}{L_d} & -\dfrac{R_d}{L_d} \end{bmatrix},$$
$$B_a = \begin{bmatrix} 0 & 0 & \dfrac{G_a}{L_d} \end{bmatrix}^T,$$
$$C_a = \begin{bmatrix} -\dfrac{K_d}{m_s} & -\dfrac{C_d}{m_s} & \dfrac{Bl}{m_s} \end{bmatrix}. \quad (4)$$

2.2 Uncertainty model

In this subsection, we draw uncertainties of the shaker plant. First of all, the physical parameters of the plant include uncertainties whose perturbation ranges are shown in Table 1.

We first describe the uncertainties of the electorical part of the shaker system. When the equivalent circuit of the drive coil is considered, the transfer function from the input voltage $G_a u_m$ to the current I_1 is represented as $1/(L_d s + R_d)$. However, it is hard to accurately describe its characteristics. We thus model the perturbation as an unstructured additive uncertainty. Here, the uncertainty weighting function W_d is selected so that it covers all the model perturbations as follows (Fujita et al., 1995):

$$W_d = 0.11 \cdot \frac{s + 500 \cdot 2\pi}{s + 100 \cdot 2\pi}. \quad (5)$$

The additive perturbation for the amplifier gain is represented as

$$\tilde{G}_a = G_a + w_g \delta_g, \quad \delta_g \in [-1, \ 1] \quad (6)$$

where $\tilde{G}_a$ denotes the actual parameter; and w_g, the weighting coefficient. The multiplicative output perturbation of the magnetic flux density is represented as

$$\tilde{B} = (1 + w_b \delta_b) B, \quad \delta_b \in [-1, \ 1], \quad (7)$$

where $\tilde{B}$ denotes the actual parameter; and w_b, weighting coefficient.

Since accurate identifications of m_s, K_d and C_d are difficult, uncertainties of the mechanical part also need to be taken into account. The transfer function of the mechanical part is represented as $1/(m_s s^2 + C_d s + K_d)$. Let us now consider the multiplicative output uncertainty caused by the parameter perturbation. Here, the uncertainty is modeled as an unstructured uncertainty, and the magnitude of the uncertainty weighting function W_m selected so as to cover all the perturbations as follows:
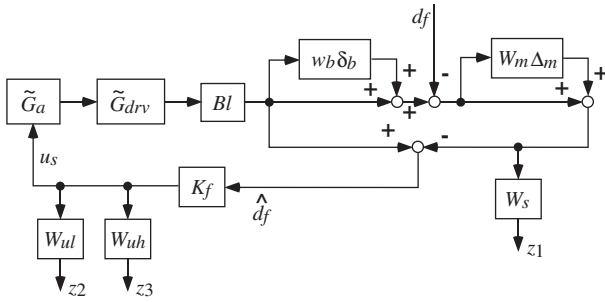
Fig. 3. Feedback structure to design the disturbance-force compensator.

$$W_m = 0.009 \cdot \frac{s + 3 \cdot 2\pi}{s + 7 \cdot 2\pi} \cdot \frac{s + 300 \cdot 2\pi}{s + 7 \cdot 2\pi}. \tag{8}$$

3. FEEDBACK CONTROLLER DESIGN

3.1 Control objectives

In this section, we design a controller to maintain robust stability against the aforementioned uncertainties and to suppress the effect of a disturbance force. A robust controller for this system is thus designed with μ–synthesis, which has many applications such as (Fujita et al., 1995). It should be noted that the control error increases in case of a large gap between the plant mpdel and its actual characteristics. To reduce the mismatch, we use a disturbance-force compensator.

3.2 μ–synthesis

Let us consider the feedback structure shown in Fig. 3, where the block K_f denotes the disturbance-force compensator. The weighting function W_s is designed so as to reflect a desirable suppression performance of the disturbance force. Note that, to improve this performance, the gain of the control frequency band is required to be enlarged within obtaining robust stability. Taking account of the issues, W_s is now chosen as

$$W_s = 2.9 \cdot \frac{14 \cdot 2\pi}{s + 14 \cdot 2\pi} \cdot \frac{70 \cdot 2\pi}{s + 70 \cdot 2\pi} \cdot \frac{140 \cdot 2\pi}{s + 140 \cdot 2\pi}$$
$$\cdot \frac{s}{s + 2.4 \cdot 2\pi} \cdot \frac{s}{s + 0.56 \cdot 2\pi}. \tag{9}$$

The magnitude of the controller is also required to be small at the high frequency band due to a low signal-to-noise ratio of the displacement response signal at the domain. A weighting function W_{uh} is thus chosen as

$$W_{uh} = 2000 \cdot \frac{s + 2.5 \cdot 2\pi}{s + 4000 \cdot 2\pi}. \tag{10}$$

On the other hand, the signal-to-noise ratio of the acceleration response signal is low at low frequency. Thus, the magnitude of the controller is required to be made small at the low frequency band. To reflect the specification a weighting function W_{ul} is designed as

$$W_{ul} = 0.9 \cdot \frac{s^2 + 2.5 \cdot 2\pi\sqrt{2}s + (2.5 \cdot 2\pi)^2}{s^2 + 0.002 \cdot 2\pi\sqrt{2}s + (0.002 \cdot 2\pi)^2}. \tag{11}$$

In summary, the generalized plant P including all the control objectives and specifications is constructed and
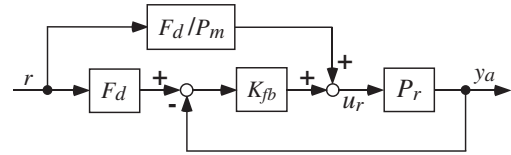

Fig. 4. Block diagram of general 2-DOF control.

the problem is successfully reduced to the μ–synthesis framework. The block structure of the uncertainty Δ is defined as

$$\Delta := \left\{ \mathrm{diag}\left(\delta_g, \delta_b, \Delta_d, \Delta_m, \Delta_p\right), \delta_g \in \mathcal{C}^{1 \times 1}, \right.$$
$$\delta_b \in \mathcal{C}^{1 \times 1}, \Delta_d \in \mathcal{C}^{1 \times 1}, \Delta_m \in \mathcal{C}^{1 \times 1}, \tag{12}$$
$$\left. \Delta_p \in \mathcal{C}^{1 \times 3} \right\},$$

where $|\delta_g| \leq 1$, $|\delta_b| \leq 1$, $|\Delta_d| \leq 1$, $|\Delta_m| \leq 1$, $\|\Delta_p\|_\infty \leq 1$, and Δ_p is a fictitious uncertainty block for robust performance.

As a result, a μ-controller is obtained after 2 iterations through the D-K iteration procedure. Then we conduct model reduction to the resulting original controller and its degree is reduced from 47 to 15.

4. FEEDFORWARD CONTROLLER DESIGN

4.1 Overview of feedforward control

In this section, we design a feedforward controller and complete the 2-DOF controller as in Fig. 4 to improve its transient response to the reference signal (Sugie and Yoshikawa, 1986). The block F_d represents the reference model; P_m, the nominal model of the plant; and P_r, the actual plant, respectively. This control system has an advantage in that the transfer function P_{yr} from the reference r to the response displacement y_a can be determined by F_d irrespective of the choice of the feedback controller K_{fb}. If the nominal model is perfect, i.e., if $P_m = P_r$, then the transfer function becomes $P_{yr} = F_d$. In addition, even in the presence of model uncertainties, as long as the feedback control works precisely, P_{yr} is maintained close to F_d.

Let us now consider a coprime factorization of P_m as

$$P_m = \frac{N_m}{M_m}, \quad N_m X_m + M_m Y_m = 1, \tag{13}$$

where N_m, M_m, X_m and Y_m are stable and proper respectively. Note that if we set $F_d = N_m$, the block F_d/P_m in Fig. 4 is replaced by M_m. We next describe the state-space model of P_m as

$$\dot{x}_m = A_m x_m + B_m u_m, \quad y_m = C_m x_m, \tag{14}$$

where $A_m = C_a{}^{-1} A_a C_a$, $B_m = C_a{}^{-1} B_a$, $C_m = C_a{}^{-1} C_a$. Then, it is known (Doyle et al., 1992) that a coprime factorization of P_m i.e. N_m, M_m, X_m and Y_m are given in the form of

$$N_m = C_m \left(sI - (A_m - B_m K_m)\right)^{-1} B_m,$$
$$M_m = 1 - K_m \left(sI - (A_m - B_m K_m)\right)^{-1} B_m, \tag{15}$$
$$X_m = K_m \left(sI - (A_m - H_m C_m)\right)^{-1} H_m,$$
$$Y_m = 1 + K_m \left(sI - (A_m - H_m C_m)\right)^{-1} B_m,$$

where K_m is a real matrix such that $A_m - B_m K_m$ is stable and H_m is a real matrix such that $A_m - H_m C_m$ is stable.
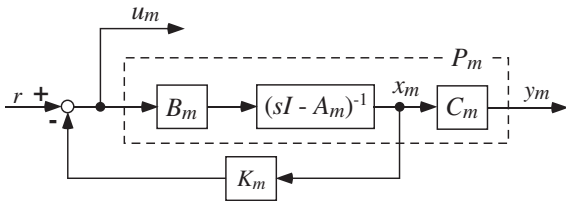
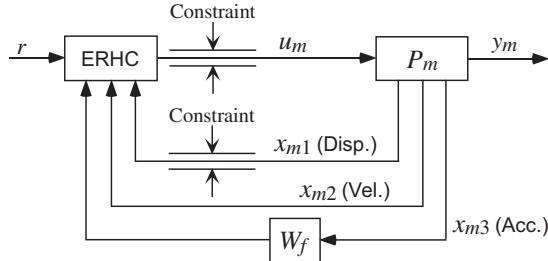Fig. 5. Block diagram to design the state feedback control

Fig. 6. Block diagram of the prediction model

Namely, M_m is represented as the transfer function from r to u_m and N_m is the transfer function from r to y_m for the closed system consisting of the plant model P_m and a stabilizing state feedback controller as shown in Fig. 5. This implies that the selection of $F_d = N_m$ is reduced to the design problem of an appropriate stable feedback controller and the block F_d/P_m is then automatically determined by the resulting M_m.

4.2 Design of ERHC preview control

The main idea of the present control scheme is to use the ERHC controller as the state feedback controller in Fig. 5 in order to generate the (modified) reference signals taking account of the displacement constraints. This scheme avoids the main drawback of the receding horizon control of requiring state feedbacks since the controller in our scheme just feedbacks the fictitious states of the plant model. The resulting block diagram of the feedforward controller is illustrated in Fig. 6.

The receding horizon control directly includes the constrains of the control input and the displacement response into the finite-time optimal control problem to be solved at each time instant. Here, the constraints are formulated as

$$-0.002 \leq x_{mk1}(k) \leq 0.002, \qquad (16)$$
$$-5 \leq u_{mk}(k) \leq 5. \qquad (17)$$

The cost function of the optimal control problem is formulated so that the acceleration shows a good tracking to the reference signals. However, using directly the acceleration as the control output and minimizing the tracking error measured by L_2-norm yields a high gain almost equal to 0 [dB] in low frequency band. In order to decrease the gain, we insert the weighting function

$$W_f = \frac{s^2 + \sqrt{2} \cdot 2\pi s + (2\pi)^2}{s^2 + \sqrt{2} \cdot 2\pi \cdot 0.01 s + (2\pi \cdot 0.01)^2}, \qquad (18)$$

and let its output be the controlled output. Then, the output response has the gain almost equal to 0 [dB] in low frequency band, which means a low gain in the acceleration response. Each weighting matrices Q_y and R_u on the
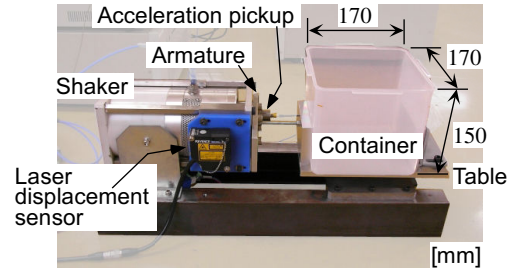

Fig. 7. Overview of experimental setup.

tracking error and the input magnitude are chosen as $Q_y = 1000$ and $R_u = 1$ respectively through trial and error processes so that the reference signal can be replicated. Note that we use L_2-norm as a metric of the size of signals. The prediction horizon H is set as $H = 10$.

We finally formulate the prediction model. In this paper, we integrate preview control with the receding horizon control scheme in order to improve the tracking performances. For this purpose, we introduce a preview model of the reference signal, which is formulated as (Katayama et al., 1985):

$$\begin{bmatrix} x'_{mk}(k+1) \\ x_{rk}(k+1) \end{bmatrix} = \begin{bmatrix} A'_{mk} & 0 \\ 0 & A_{rk} \end{bmatrix} \begin{bmatrix} x'_{mk}(k) \\ x_{rk}(k) \end{bmatrix} +$$
$$\begin{bmatrix} B'_{mk} \\ 0 \end{bmatrix} u_{mk}(k), \qquad (19)$$
$$x_{rk}(k) = \begin{bmatrix} r_k(k) \\ \vdots \\ r_k(k + N_L - 1) \end{bmatrix},$$
$$A_{rk} = \begin{bmatrix} 0 & 1 & & 0 \\ & 0 & \ddots & \\ & & \ddots & 1 \\ 0 & & & 1 \end{bmatrix},$$

where it is noticed that each parameter is discretized and N_L denotes the number of the preview information.

By integrating the reference model and weighting function W_f with the discretized nominal plant model P_m, we can formulate the prediction model. Then, we compute an appropriate ERHC controller by solving offline the constraint optimal control problem with the cost function of evaluating the error between the output of W_f and the reference waveform and the model constraints, displacement constraints (16) and input constraints (17). In this paper, we use MATLAB/Simulink and MPT 2.6.2 (Kvasnica et al., 2004), for the design.

5. CONTROL RESULT

5.1 Experimental setting

The control performance is demonstrated through experiments using the system shown in Fig. 7. A covered container with water is employed as the specimen for the excitation experiment, and a sloshing, which is liquid vibration, is occurred by executing the container. The size of rectangular-type container is 170 mm $\times$ 170 mm $\times$ 150 mm (length, width, height). These controllers are basically
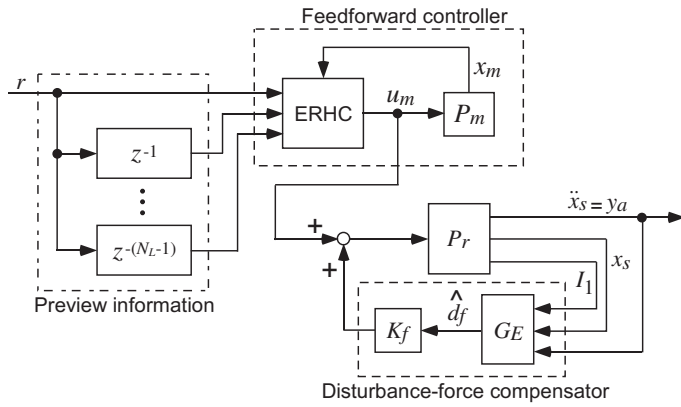
Fig. 8. Block diagram of the experimental system

discretized via the Tustin transform at the sampling frequency of 512 Hz. Since it is difficult that the disturbance force is directly measured, the disturbance force is estimated using the displacement and acceleration responses of the armature and the current response of the drive coil. As shown in this figure, the estimated disturbance force $\hat{d}_f$ is given as follows,

$$\hat{d}_f = BlI_1 - K_d x_s - \left(m_s + \frac{C_d}{s + \omega_p} \right) \ddot{x}_s, \qquad (20)$$

where ω_p denotes the adjustment parameter to keep the gain low in a low frequency band. Note that though the gap between the estimates and the actual disturbance force is inevitable, the estimation error is expected to be suppressed by the feedback controller.

The block diagram of the experimental system is illustrated in Fig. 8, and the block enclosed by the chained line is the generator of the preview information.

5.2 Experimental results

This experiment is executed by using a real waveform data of earthquakes as the reference signal. The control performance is evaluated by the acceleration tracking errors together with constraint fulfillment on the rated displacement. In this experiment, it is assumed that the range of the rated displacement is set from -2 mm to 2 mm as in (16).

We first implement the ERHC controller in the absence of preview information of the reference. The acceleration response is shown in Fig. 9 and the displacement response is shown in Fig. 10. We see that the displacement response is certainly lie in the limitation, which demonstrates the effectiveness of the ERHC controller as a control scheme of constrained systems. The acceleration response is in part consistent with the reference signal but the rms error (= rms value of the error signal / rms value of the reference signal × 100 %) is given by 57.7 % and it is bit larger than the acceptable level.

Next, the present preview ERHC controller is implemented, whose results are shown in Fig. 11 and Fig. 12. The number of the preview information is set as $N_L = 16$. Since, in case of $H < N_L$, the advantage of using the preview information is lost. the prediction horizon is set at $H = N_L$ in the experiment. Furthermore, because of extending the target period of the preview control the
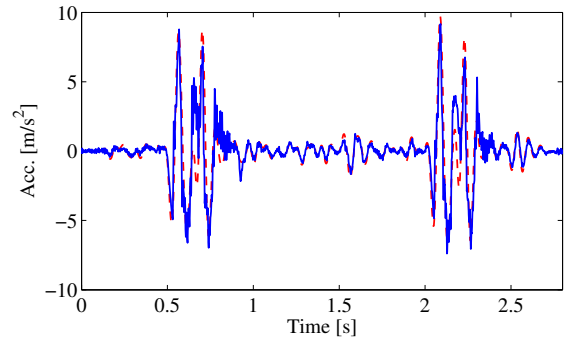

Fig. 9. Results of the acceleration response without the preview control. The reference is indicated by the dashed red line and the response is indicated by the solid blue line.
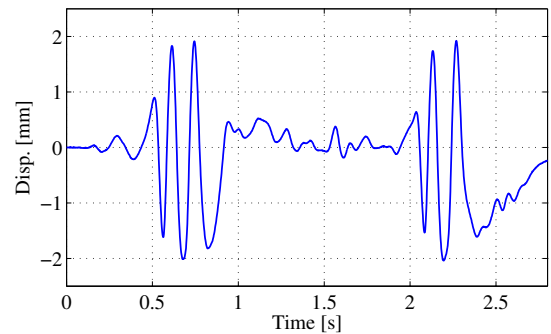

Fig. 10. Displacement response with the preview control.

Table 2. The rms error when the number of the preview information is changed.

Sampling frequency	Rms error		
	$N_L = 1$	$N_L = 8$	$N_L = 16$
512 Hz	57.7 %	53.8 %	40.6 %
256 Hz	70.5 %	37.9 %	30.6 %

sampling frequency of the feedforward controller is reduced to half. We see from the figures that the proposed controller yields a good performance, namely the acceleration response is consistent with the reference signal except for the period when the reference exceeds the displacement limitation. The value of the rms error is also reduced to 30.6 %. In addition, the displacement response is also constrained within the limited range.

The rms errors for a variety of the number of the previews are listed in Table 2, where we examine two different sampling frequencies of the feedforward controller. We see from the list that the rms error decreases as N_L increases. The result shows the value of the preview information more explicitly and the validity of the present control scheme.
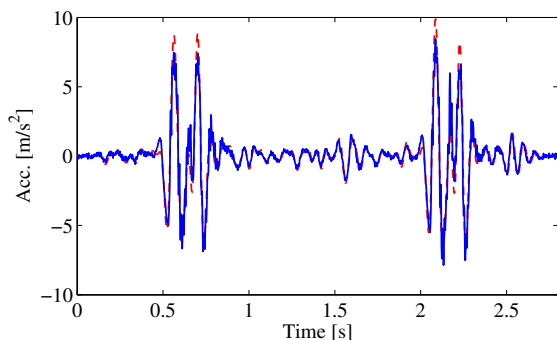
Fig. 11. Results of the acceleration response using the preview controller. The reference is indicated by the dashed red line and the response is indicated by the solid blue line.
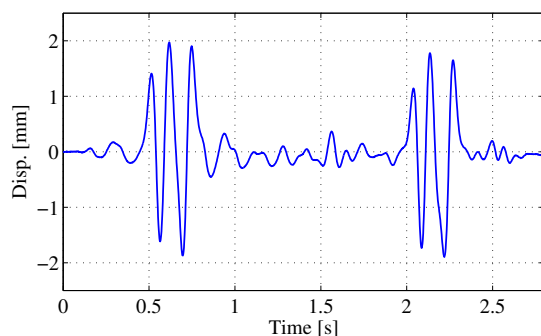

Fig. 12. Displacement response with the ERHC controller.

6. CONCLUSION

In this paper, a preview controller using an ERHC was presented for control of electrodynamic shaker systems. In order to compensate for a variety of uncertain effects, a disturbance force compensator was employed. Furthermore, to improve the tracking performance, a preview control scheme based on ERHC was introduced in the feedforward controller design of the 2DOF control mechanism. Experiments were performed using a tedtbed of an electrodynamic shaker, and the effectiveness of the present control scheme was confirmed.

REFERENCES

R. de Callafon, R. Nagamune, and R. Horowitz. Robust dynamic modeling and control of dual-stage actuators. *IEEE Transactions on Magnetics*, 42(2):247–254, 2006.

J. C. Doyle, B. A. Francis, and A. R. Tannenbaum. *Feedback control theory*. Macmillan Publishing, 1992.

M. Fujita, T. Namerikawa, F. Matsumura, and K. Uchida. μ–synthesis of an electromagnetic suspension system. *IEEE Transactions on Automatic Control*, 40(3):530–536, 1995.

T. Hatanaka, T. Yamada, M. Fujita, S. Morimoto, and M. Okamoto. Explicit receding horizon control of automobiles with continuously variable transmissions. In *Proc. of International Workshop on Assessment and Future Directions of Nonlinear Model Predictive Control*, pages PI–2, 2008.

M. Iwasaki, K. Ito, M. Kawafuku, H. Hirai, Y. Dozono, and K. Kurosaki. Disturbance observer-based practical control of shaking tables with nonlinear specimen. In *Proc. of the 16th IFAC World Congress on Automatic Control*, Prague, Czech, July 2005.

Z. Jamaludin, H. Van Brussel, and J. Swevers. Design of a disturbance observer and model-based friction feedforward to compensate quadrant glitches. In *Motion and Vibration control*, pages 143–154. Springer, 2009.

T. Katayama, T. Ohki, T. Inoue, and T. Kato. Design of an optimal controller for a discrete-time system subject to previewable demand. *International Journal of Control*, 41(3):677–699, 1985.

M. Kvasnica, P. Grieder, and M. Baotić. Multi-Parametric Toolbox (MPT), 2004. URL http://control.ee.ethz.ch/ mpt/.

C. Lauwerys, J. Swevers, and P. Sas. Robust linear control of an active suspension on a quarter car test-rig. *Control Engineering Practice*, 13:577–586, 2005.

D. P. Stoten and N. Shimizu. The feedforward minimal control synthesis algorithm and its application to the control of shaking-tables. *Proceedings of the Institution of Mechanical Engineers, Part I: Journal of Systems and Control Engineering*, 221(3):423–444, 2007.

T. Sugie and T. Yoshikawa. General solution of robust tracking problem in two-degree-of-freedom control systems. *IEEE Transactions on Automatic Control*, 31(6): 552–554, 1986.

U. Uchiyama and M. Fujita. Robust disturbance-force compensator for time waveform replication of an electrodynamic shaker. *JSME Journal of System Design and Dynamics*, 4(1):1–12, 2010.

U. Uchiyama, T. Hatanaka, and M. Fujita. 2dof control of an electrodynamic shaker using explicit receding horizon control for feedforward term. In *CCA component on the IEEE 2010 MSC*, pages 596–601, 2010.

K. Yano and K. Terashima. Robust liquid container transfer control for complete sloshing suppression. *IEEE Transactions on Control Systems Technology*, 9(3):483–493, 2001.

J. Zimmermann and O. Sawodny. Modeling for simulation and control od a x-y high precision positioning table. In *Proc. of the 3rd Annual IEEE Conference on Automation Science and Engineering*, pages 1093–1098, Scottsdale, USA, September 2007.